

is kept as vertical. The process is repeated when the antenna is covered with radomes along with ground plane. Radiation patterns are plotted using pattern recorder on the same chart for comparison. The whole process is carried out for both L_1 and L_2 antennas and for both polarizations.

Two circularly polarized circular patch antennas are designed and fabricated at L_1 and L_2 frequencies using RT-5880 substrate ($\epsilon_r = 2.2$, $h = 1.6$ mm) by adopting photolithographic process. Vertical ground planes are designed taking beamwidth of the antennas and cut-off angles for multipath rejection into consideration. GFRP radomes are designed to cover the antennas. The vertical ground planes are embedded into radomes to give more mechanical strength and firm fixing into the antenna. The mounting configuration of the antenna with radomes and vertical ground plane is shown in Figure 4. Return loss measurements of the antennas are carried out using network analyser and are found to be less than 20 dB at resonance frequencies of the two antennas. Radiation pattern measurements were carried out in an RF anechoic chamber for the two antennas (Figures 3 and 4). Initially, the radiation pattern of the antenna is plotted without the presence of the vertical ground planes and radomes. Later the ground planes and radomes are integrated with the antenna and the measurements were repeated. The patterns are superimposed on the same chart for easy comparison of the performance of the antenna with and without the presence of ground plane and radome. The typical radiation patterns of L_1 and L_2 antennas with and without the presence of ground planes and radomes are given in Figure 5. From the radiation pattern plots it is found that the transmission loss of the radome is 1 dB (90% transmission) for both the antennas. The half power beamwidth of the antenna in the presence of radome and ground plane increased by 10% (80 to 88° and 75 to 83° for L_1 and L_2 respectively). Variation in gain in the operating band is only 0.5 dB. Beam sharpening by 3 and 4 dB at the lower elevation angles for L_1 and L_2 respectively is achieved.

Various multipath rejection techniques are discussed and compared. A technique based on vertical ground plane is developed to reject multipath signals entering the GPS receiving antenna through low elevation angles above and below the horizon. The technique is validated with design and development of two circular patch antennas with vertical ground planes. Experimentation is carried out on these two circular polarized patch antennas at L_1 and L_2 frequencies with vertical ground planes and radomes. At low elevation angles ($\pm 5^\circ$), beam sharpening takes place, which will help in rejecting multipath signals. Beamwidth of the antennas is improved significantly by 10%.

3. Pasetti, A. and Glulichchi, L., Experimental results on three multipath compensation techniques for GPS-based attitude determination. American Astronautical Society (AAS 99-013), 3–7 February 1999.
4. Counselman, C. C., Multipath rejecting GPS antennas. *Proc. IEEE*, 1999, **87**, 86–91.
5. Bhal, I. J. and Bhartia, P., *Microstrip Antennas*, Artech House, New York, 1980.
6. Garg, R., Bhartia, P. and Inder Bahl, *Microstrip Antenna Design Hand Book*, Artech House, New York, 2001.
7. Walton, J. D., *Techniques of Radomes Design*, McGraw Hill, New York, 1970.

ACKNOWLEDGEMENTS. We thank G. Kumarswamy Rao, Director, DLRL for interest in this work. Thanks are also due to Dr V. Misra, for his constant encouragement.

Received 21 May 2005; revised accepted 3 November 2005

Study of high-resolution satellite geoid and gravity anomaly data over the Bay of Bengal

T. J. Majumdar¹, K. S. Krishna^{2,*}, S. Chatterjee¹, R. Bhattacharya¹ and Laju Michael²

¹Marine and Water Resource Group, Remote Sensing Applications Area, Space Applications Centre, Indian Space Research Organization, Ahmedabad 380 015, India

²Geological Oceanography Division, National Institute of Oceanography, Dona Paula, Goa 403 004, India

Geoid and gravity anomalies derived from satellite altimetry are gradually gaining importance in marine geo-scientific investigations. Very high-resolution gravity database generated from Seasat, Geosat GM, ERS-1 and TOPEX/POSEIDON altimeters data of the northern Indian Ocean, has been used in the preparation of geoid and free-air gravity maps. In the present work, we have investigated various products of satellite data of the Bay of Bengal, thereby correlated to known plate tectonic feature (Sunda subduction zone), volcanic traces (Ninetyeast and 85°E ridges) and continental margin features. Besides, Swatch of No Ground and modified continental slope due to sediment discharge from East Coast rivers are some of the finer structures observed in free-air gravity anomaly data. Furthermore, the data are compared with ship-track gravity anomalies along 14.64°N lat. for their consistencies and interpreted under the constraints of seismic results for understanding the evolution of structural features of the region. Two different wavelength (100–200 and 200–500 km) components derived from satellite gravity anomaly data have been studied to explain the geophysi-

1. Parkinson, B. W. and Spilker, J. R., *Global Positioning System: Theory and Application*, American Institute of Aeronautics and Astronautics, Washington DC, 1996.

2. Hannah, B. M., Modeling and simulation of GPS multipath propagation, Ph D thesis, Queensland University of Technology, Australia, 2001.

*For correspondence. (e-mail: krishna@nio.org)

cal anomalies associated with the Ninetyeast and 85°E ridges and two isolated structures in terms of isostatic compensation due to their loads with respect to the already evolved lithosphere. It is found that the magnitude of the flexure at crust–mantle boundary beneath the 85°E Ridge and structural high close to the margin is relatively higher than that of the Ninetyeast Ridge.

Keywords: Compensation mechanism, geoid and gravity anomaly data, lithospheric flexure, Ninetyeast and 85°E ridges, satellite altimetry.

In recent years satellite altimetry has emerged as a powerful reconnaissance tool for exploration of sedimentary basins on continental margins as well as in deep-water regions^{1,2}. With the advent of more altimetric missions, with increasing accuracies and varying orbital configurations, it has become possible to generate large-scale altimeter-derived residual geoid and gravity anomaly maps over the oceans. With ERS-1 168-day repeat altimeter data, a database had been earlier generated across the Indian offshore regions with cross-track resolution as high as 16 km^{2,3}. However, with the availability of very-high resolution Geosat GM (Geodetic Mission) data along with Seasat, ERS-1 and TOPEX/POSEIDON altimeter data, it is now possible to generate a very high-resolution data with a grid of around 3.33 km^{4,5}. The data would be helpful in extraction of minute details from geoid and gravity maps of the Indian offshore. The basic concept of the technique lies in the fact that the surface of any water body, in absence of external forces, forms an equipotential surface. The sea-surface height measured by satellite altimeter when corrected for atmospheric propagation delays and dynamic oceanic variabilities conforms to the equipotential surface, known as the geoid (Figure 1). The geoid contains information regarding mass distribution inside the earth, including those due to sharp changes in seafloor topography. The geoid is used to compute residual and prospecting geoids – hypothetical surfaces related to mass distributions within the lithosphere⁶.

In the present work we have used high-resolution gravity database generated from Seasat, Geosat GM, ERS-1 and TOPEX/POSEIDON altimeters data of the Bay of Bengal. The datasets are more accurate and detailed (off-track resolution about 3.33 km and grid size about 3.5 km) compared to ERS-1 (168-day repeat) altimeter data (off-track resolution about 16 km and grid size about 20 km). In this work, we have investigated various products of satellite data of the Bay of Bengal for (i) generation of high resolution classical and residual geoids and related gravity anomalies over a part of the eastern Indian offshore in ARCGIS environment, (ii) validation of high resolution satellite gravity with ship-borne gravity, and (iii) use of high-resolution altimeter-derived geoid/gravity anomaly maps over the eastern Indian offshore region for understanding the evolution of subsurface features.

The sea surface height (SSH) with respect to the reference ellipsoid is computed for instrumental bias and atmospheric propagation delays. It is a fundamental geophysical parameter used for various oceanographic and geophysical studies⁷.

$$\text{Sea surface height (SSH)} = \text{Orbit height (H)} - \text{Corrected altimetric range (h')}. \quad (1)$$

The SSH observed by the altimeter is only an instantaneous sea surface topography and deviations of SSH from the geoid are due to various dynamic variabilities, e.g. ocean tide, solid tide, electromagnetic bias, inverse barometric pressure effect, etc.

Fast Fourier Transform (FFT) approach uses geoid for computation of free-air gravity anomaly⁸. The approach is based on a flat earth approximation and is derived from the two fundamental equations, namely the Brun's equation and the equation of physical geodesy^{9,10}. The relation between gravity anomaly and geoid undulation derived from the above two fundamental equations was given by Chapman⁸:

$$F(\Delta g) = g_0 |k| F(N), \quad (2)$$

where $F(\Delta g)$ is the Fourier transform of free-air gravity anomaly, $F(N)$ the Fourier transform of geoid undulation and $|k|$ the one-dimensional wavenumber associated with wavelength λ .

The geoid, residual geoid and gravity anomaly data are prepared for the region bounded by lat. 5 and 25°N, and long. 80 and 95°E in the northeastern Indian Ocean (Figure 2 a–c respectively). (For security reasons position coordinates have been omitted in satellite gravity maps.)

Different spectral components of geoid and free-air gravity anomalies correspond to varied magnitude geological features lying at different depth levels. Accordingly,

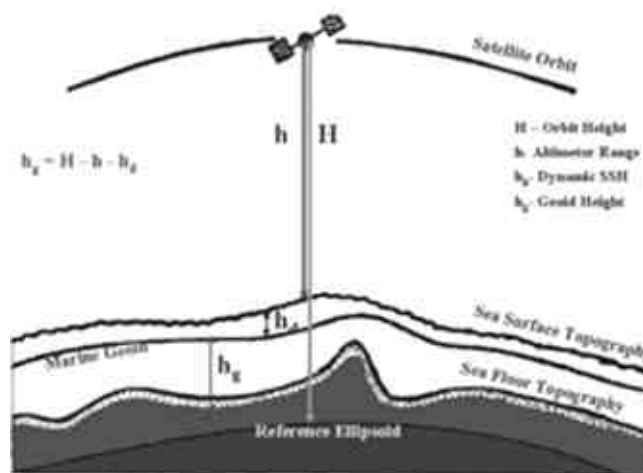


Figure 1. Basics of satellite altimetry after Fu *et al.*³⁶.

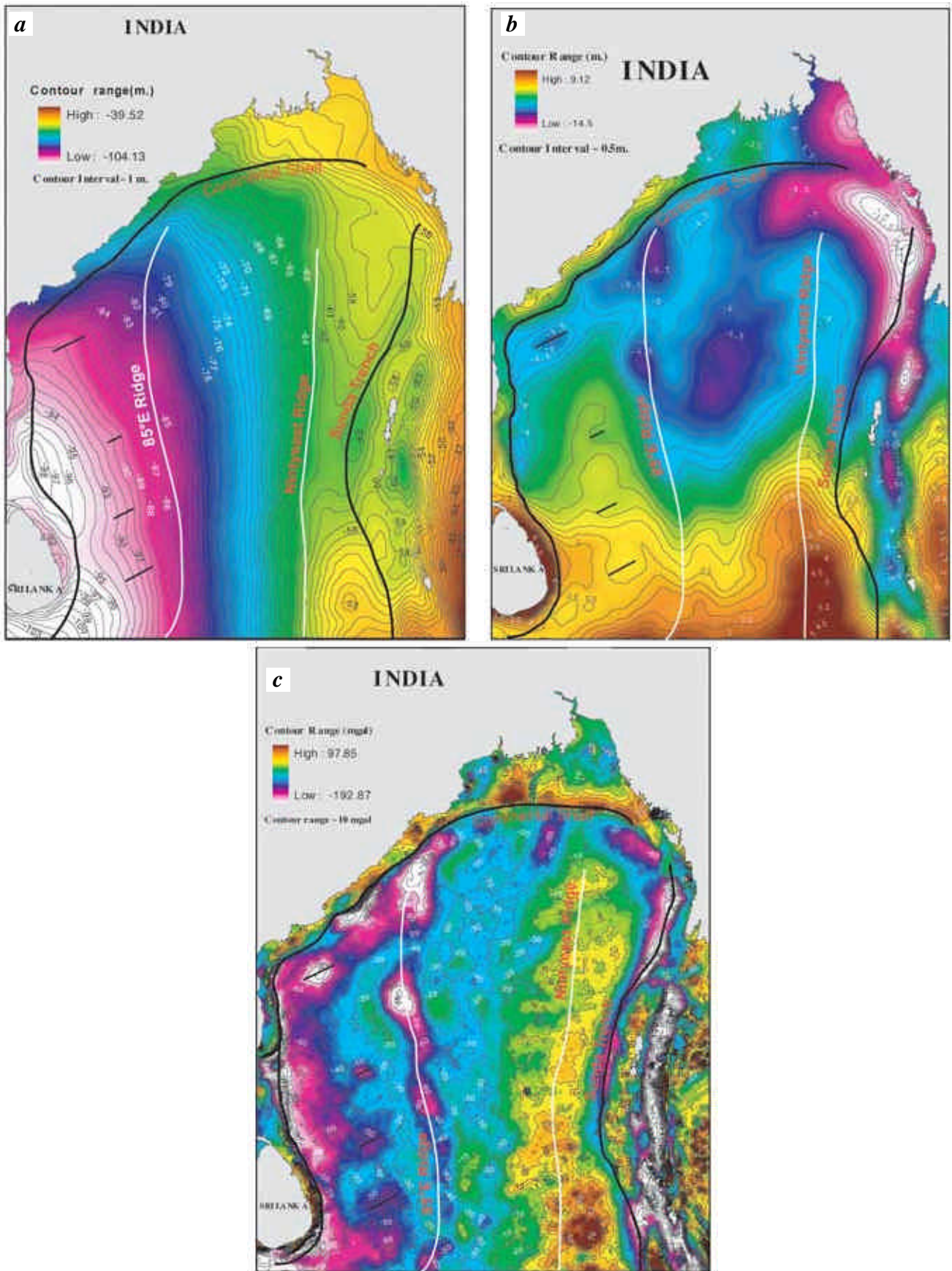


Figure 2. Geoid data (a), residual geoid anomaly (b) and free-air gravity anomaly data (c) of the Bay of Bengal derived from satellite altimetry.

the residual geoid and gravity anomaly data of the Bay of Bengal are segmented into intermediate and long-wavelength spectral components¹¹. Long-wavelength component (200–500 km) mainly reflects the undulations at crust–mantle boundary, whereas intermediate-wavelength component (100–200 km) is expected to bring out the details of lateral variations between basement topography and continental-rise sediments. The information thus obtained can be used to outline the tectonic trends and for understanding the isostatic compensation of several geological structures at different depths.

The evolution of the eastern Indian Ocean started with the break up of eastern Gondwanaland into two separate continental masses, Australia–Antarctica and Greater India, in the Early Cretaceous^{12–14}. Elan Bank, a micro-continent, which presently lies on the west margin of the Kerguelen Plateau in the southern Indian Ocean, got detached from the eastern margin of India¹⁵ at about 120 Ma. Thus the eastern margin of India had witnessed two continental break ups in early stages of eastern Gondwana splitting. During the process, the ocean has experienced three major phases of seafloor spreading: initially moved in NW–SE direction, secondly drifted in N–S direction and finally continuing in NE–SW direction. The lithospheric plates (Indian, Australian and Antarctica) in the Indian Ocean were reorganized at three geological ages in the past. During the mid-Cretaceous (95 ± 5 Ma), Australia had separated from Antarctica^{12,16}. The second major plate reorganization occurred during the middle Eocene and resulted in merging of the Australian and Indian plates as a single Indo-Australian plate^{17,18}. Subsequently, at late Miocene age, high magnitude seismicity and lithospheric deformation in the central Indian Ocean have contributed to the development of a new diffuse-type plate boundary within the traditionally believed Indo-Australian plate^{19–22}.

Marine geophysical measurements from ship-borne platforms over the Bay of Bengal have imparted valuable information on structural fabric and nature of the crust, which have significantly contributed to the understanding of the evolution of the region. Two linear features (Ninetyeast and 85°E ridges) emplaced by the Kerguelen and Crozet hotspots, respectively sit longitudinally on the early Cretaceous oceanic crust of the Bay of Bengal. The ridges divide the Bengal Fan into two basins: Western Basin between eastern margin of India and the 85°E Ridge and Central Basin between the ridges²³. The Rajmahal traps erupted by the Kerguelen hotspot at ~118 Ma are found in the Bengal Basin, while the Sylhet traps formed at ~107 Ma are found in the Mahanadi Basin²⁴. Despite the fact that the crust in the Bay of Bengal is oceanic in nature, from magnetic anomaly studies two different ages (132 and 120 Ma) were assigned to the earliest oceanic crust^{14,25,26}. Subsequently, Krishna and Gopala Rao²⁷ have supposed that the oceanic crust of the Bay of Bengal needs to have traces of earlier spreading centres that ceased at 90–95 Ma and presence of transferred crust

of the Antarctica plate. Newly identified M-sequence anomalies (both sets of M9Ny – M2o) in the Enderby Basin, off Antarctica, suggest¹⁵ that the Elan Bank was detached from India no earlier than 124 Ma. These results imply that most part of the oceanic crust in the Bay of Bengal was evolved during the Cretaceous magnetic quiet period (120–84 Ma). Hence no pronounced magnetic anomalies were observed in the Bay of Bengal^{14,16}.

A collaborative project between NIO and SAC on ‘Satellite geoid/gravity modelling for lithospheric studies’ provides an opportunity to collate two individual databases of satellite gravity and ship-borne gravity data of the Bay of Bengal. In Figure 3 we have shown the network of ship-borne gravity profiles acquired by different national and international institutions in the Bay of Bengal. We use this gravity database in the project for preparation of free-air anomaly contour map and regional-residual maps. Satellite free-air gravity data along 14.64°N lat. were compared with the ship-borne gravity data (profile Man-01) along the same latitude for the purpose of observing the consistencies and deviations between them (Figure 4). This profile was chosen as we have good control with seismic reflection data. Comparison of data reveals that both satellite and ship-borne anomalies are fairly in good agreement with some deviations of about 5 mGal, which is within the accuracy limits of the satellite free-air gravity data. Further, two major linear gravity features (Ninetyeast and 85°E ridges) are depicted significantly in both the datasets. Therefore, the satellite free-air gravity anomalies

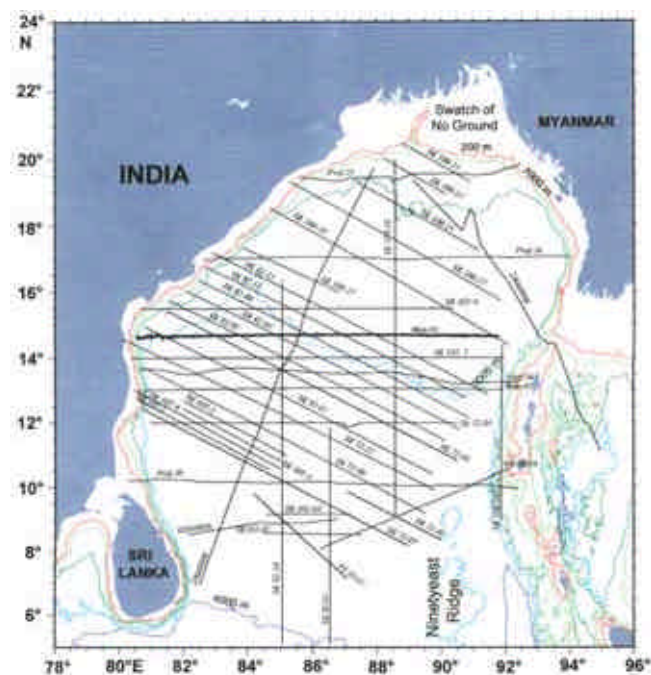


Figure 3. Ship-borne gravity profiles of the Bay of Bengal acquired on-board national and international research vessels. Solid line shows location of the profile along which interpreted seismic results and various products of satellite gravity data are shown in Figure 4.

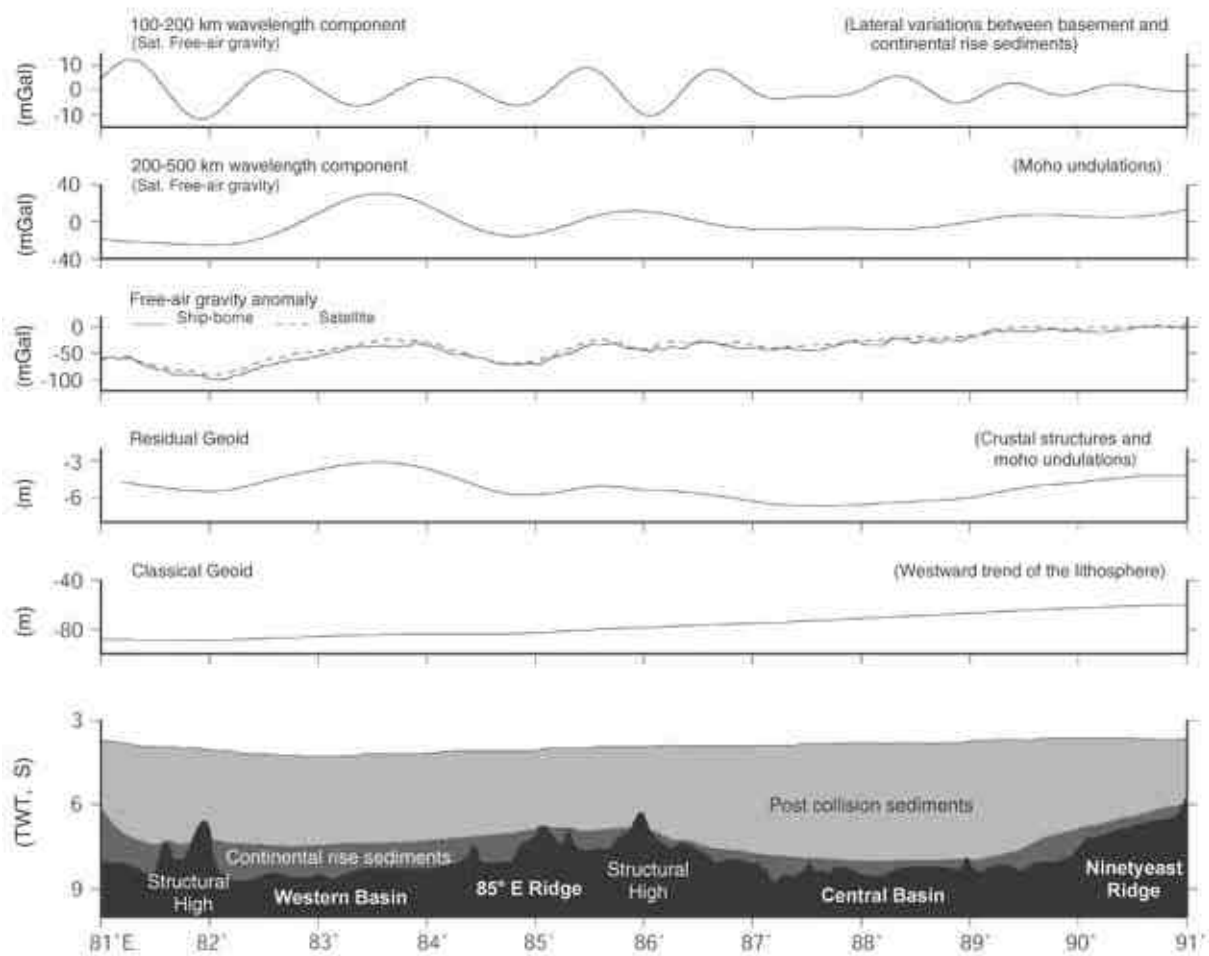


Figure 4. Comparison of anomalies and various components along profile 14.64°N. Basement topography and two sediment units separated by an Eocene unconformity are after Gopala Rao *et al.*¹⁴. Geoid, residual geoid and gravity anomalies derived from satellite altimetry are shown and compared with ship-borne gravity data for consistencies and deviations. Two different wavelength components (100–200 and 200–500 km) are also shown for understanding mass distributions at varied depth levels. Location of the profile is shown with solid line in Figure 3.

of the Bay of Bengal can be reasonably considered in mapping the structural features of the region. Thereby the results can be used to study the tectonics and related oceanic processes of the Bay of Bengal.

Basement topography and the overlying two sediment units interpreted from seismic reflection profile (Man-01) along 14.64°N lat. are shown in Figure 4. The basement in the Bay of Bengal generally consists of two major structural rises (Ninetyeast and 85°E ridges) and troughs (Western and Central basins). The structures are regionally extending in near N–S direction^{14,28–31}, which has broadly transformed the Bay of Bengal oceanic crust into alternative crests and troughs. Morphologically, the troughs are much wider than the crests. Additionally, a gentle regional-tilt of the basement is also observed towards the eastern margin of India. Even in bathymetry data similar kind of tilt is observed from east to west. Besides, two isolated structural highs (local features) are noticed near the continental margin and to the east of the 85°E Ridge. The two sedimentary units formed during the pre- and

post-collision tectonic settings are separated by the Eocene erosional unconformity^{13,14}. The pre-collision (continental-rise) sediments are relatively thicker in the Western Basin than those in the Central Basin (Figure 4). The seismic results are stacked with ship-borne gravity and satellite geoid and gravity data and their components (Figure 4) to investigate the contributions of mass distributions lying at different depths. Besides the regional structures (aseismic ridges and basins), we have also examined gravity signatures of the finer geological structures, viz. Swatch of No Ground and Krishna–Godavari Basin region (Figure 5 a, b) for understanding their evolution and contribution to regional tectonic settings.

The geoid data are generally expected to provide information on long-wavelength structural features lying at depths approximately 100 km and occasionally some of the shallow structures that have excessive mass density contrasts. The geoid height data of the Bay of Bengal (Figure 2 a) relative to the reference ellipsoid varies from –105 m in south of Sri Lanka to –40 m in southeast of the

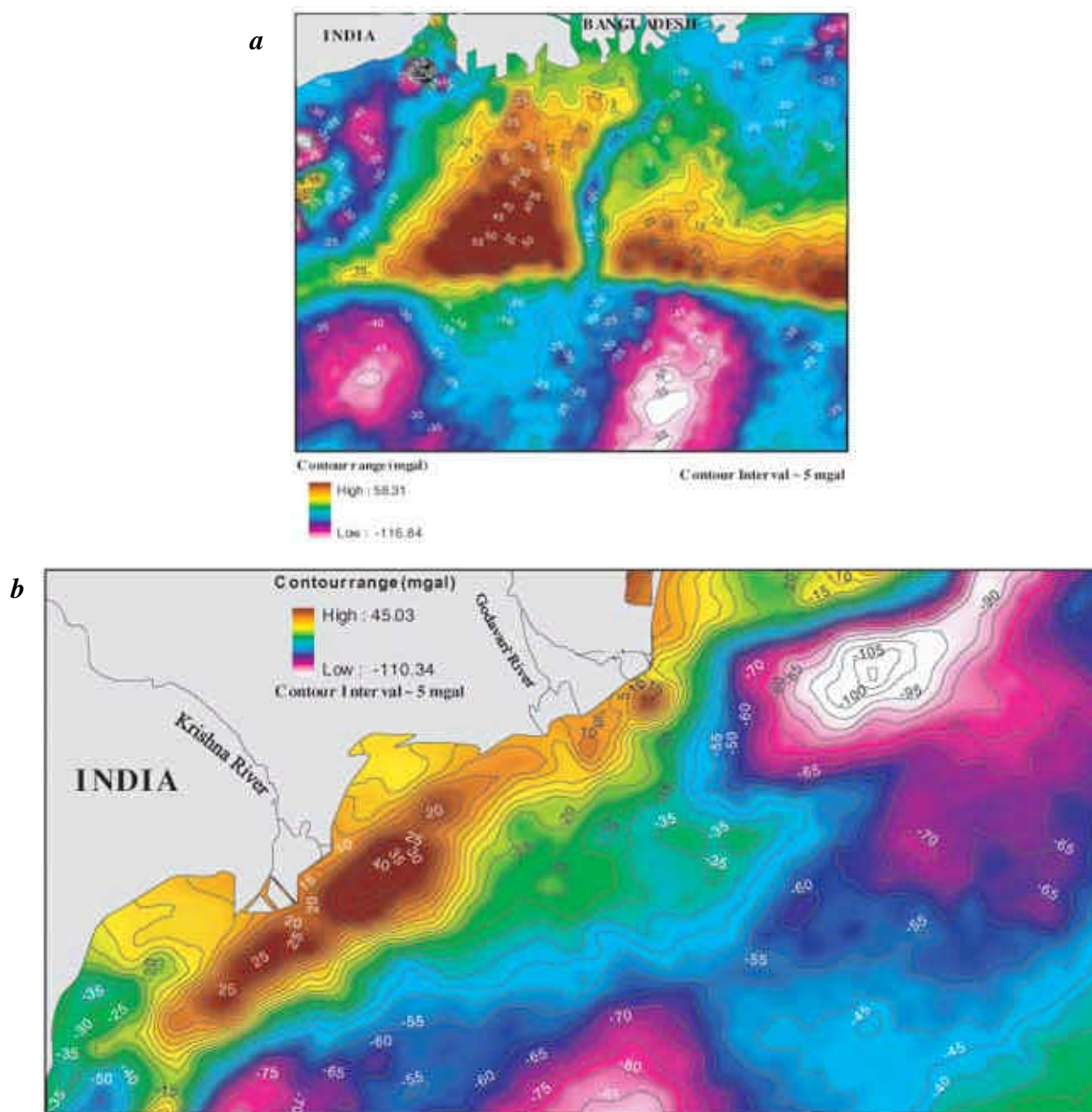


Figure 5. Satellite images of some finer structures of the Bay of Bengal. Free-air anomaly contour map of Swatch of No Ground Canyon (*a*) and Krishna–Godavari Basin (*b*).

Andaman–Nicobar Islands. This variation corresponds to general geoidal gradient of approximately 39 mm/km. Steep geoid gradients are noticed in a region between the 85°E and Ninetyeast ridges, while at the east and west of the region, the gradients are relatively gentle due to the influence of the Ninetyeast Ridge and Sunda Trench, and morphology of the continental margin, respectively. The geoid data of the Bay of Bengal can be reasonably correlated with known geological features such as the Sunda Trench (the boundary of the Indian plate against the Burmese plate) and continental shelf-slope of the eastern margin of India. Besides those, the geoidal heights are

generally dipping towards the eastern margin of India (Figures 2 *a* and 4), which is associated with regional westward tilt of the lithosphere. As the age of the oceanic lithosphere increases towards the eastern margin of India, the lithosphere cools and subsides to depths in a near linear-dipping pattern towards west. Earlier, Gopala Rao *et al.*¹⁴ observed such regional tilt in ship-borne free-air gravity data of the Bay of Bengal and attributed it due to the subsidence of oceanic lithosphere with crustal age. Short-wavelength structural details, the 85°E Ridge, the Ninetyeast Ridge and isolated basement highs are in general masked.

Residual geoidal height data are important for interpretation of geological structures within the crust and undulations of crust–mantle boundary. Hence the deeper earth effect has been removed using spherical harmonic modelling of the geopotential field³². The data thus obtained after removal of effects of long-wavelength geoid features, are predominantly associated with deep-earth mass distributions. The residual geoid data vary from -11.5 m in west of Myanmar to $+5.5$ m on east margin of the Ninetyeast Ridge at 5°N lat. (Figure 2 *b*). Relative residual geoidal lows are clearly seen associated with the Sunda Trench, 85°E Ridge and some isolated structural highs, whereas the Ninetyeast Ridge is associated with the residual geoidal high. It is also observed that residual geoid anomalies are broadly dipping towards north. The pattern was also noticed earlier by Rajesh and Majumdar³³ in ERS-1 altimeter data. They concluded that the basement trends downward and thickness of Bengal Fan sediments increases as well, as one proceeds towards north. Another notable point of interest in the data is the absence of long-wavelength geoidal feature generated by regional tilt of the oceanic crust in the Bay of Bengal. The structural high to the east of the 85°E Ridge, although its relief is higher than the other structural high and the 85°E Ridge (Figure 4), does not associate with residual geoidal low, which seems to indicate the absence of flexure at the Moho boundary below the structural high. Whereas this structural high is associated with small-amplitude low free-air gravity anomaly (Figure 4), possibly contributed by lateral density contrasts between basement rocks (structural high) and continental-rise sediments. Earlier, it was reported that all the basement rises, including the 85°E Ridge in the Bay of Bengal are associated with low gravity anomalies^{14,31,34}. The present results will add more clarity to the earlier understandings that there are some structural highs, whose amplitudes of low gravity anomalies are small, but not contributed by the flexure at the Moho boundary.

Satellite-derived free-air gravity anomaly data (Figure 2 *c*) show the prominent gravity signatures that are associated with the Sunda Trench (distinct gravity low), Ninetyeast Ridge (subdued gravity high), 85°E Ridge (distinct gravity low), continental shelf-slope of the eastern margin of India (steep gravity low) and some isolated structural highs (gravity lows marked with black solid line between eastern margin of India and the 85°E Ridge). The gravity anomalies, in general, decrease towards north in the distal Bengal Fan and towards west in the Bengal Fan as have been reported earlier^{14,21,31}, suggesting that the trends seem to be associated with the directions of paleo-plate motions. The anomalies of the Ninetyeast Ridge, 85°E Ridge and shelf edge are prominent and are seen distinctly from the regional anomalies of the Bay of Bengal. The amplitude of the gravity lows associated with the 85°E Ridge is varying along its strike from south to north (Figure 2 *c*). Along $14^{\circ}10'\text{N}$ lat. the gravity low reaches

up to -95 mGal (with a net anomaly of -70 mGal), while in the south along 7°N , the gravity low reaches up to -40 mGal (with an anomaly of about -15 mGal). It is interesting to note that both aseismic type of ridges (85°E and Ninetyeast ridges) in the central Bay of Bengal, in spite of their burial under about 3 km thick Bengal Fan sediments¹⁴, display two opposite (low and high) gravity signatures. The gravity low anomalies of the 85°E Ridge switch over to gravity highs toward south of 5°N ; the change was interpreted to coincide with termination/thinning of pre-collision continental sediments in the Bay of Bengal³¹. The enigmatic gravity low of the 85°E Ridge was explained by the underplating material and crustal root at the base of the crust²⁸. In subsequent studies the low anomaly was explained with the presence of meta-sediments, more dense than volcanic rocks, on both sides of the ridge and flexure of the lithosphere beneath it³¹. Besides these regional structures, we have also noticed steep gradient gravity anomalies on continental slope of the eastern margins of India and Sri Lanka (Figure 2 *c*). Such steep gravity anomalies were also noticed in ship-borne gravity data of the eastern margin of India²⁸. Free-air gravity anomaly data along 14.64°N lat. are segmented into long-wavelength (200–500 km) and short-wavelength (100–200 km) components (Figure 4), with a view to separate contributed sources to the gravity anomaly. The major component generally provides information on the Moho boundary. The structural high east of the 85°E Ridge is not underlain by any flexure at the Moho boundary, whereas the Ninetyeast Ridge is supported by a mild flexure at Moho boundary, suggesting that both the structures were emplaced on aged oceanic crust. The minor component possibly indicates the response of lateral density contrasts between basement rocks (structural high) and continental-rise sediments (Figure 4).

Free-air gravity anomalies of some finer structures such as Swatch of No Ground and Krishna–Godavari Basin are shown in Figure 5 *a, b*. On the Bangladesh continental shelf, 15 mGal gravity low is associated with a nearly 20 km wide and 140 km long canyon, known as Swatch of No Ground (Figure 5 *a*). Its southward continuity on the slope-surface of the Bangladesh margin is not traceable in the gravity contour map. Using morphological results of the Bengal Fan, Curray *et al.*³⁵ have mapped the canyon continuity beyond the margin up to the southern limit of upper Bengal Fan at 18°N lat. The depression in the canyon beyond the margin may get smaller in size, particularly in its depth, and thus, there are no significant gravity anomalies seen associated with the southern part of the canyon (Figure 5 *a*). The canyon is bounded by two positive anomaly closures (30 and 55 mGal) on the shelf region and two negative anomaly closures (-50 and -55 mGal) on the slope region of the margin. Along the southern part of the eastern margin of India a typical short-wavelength pronounced gravity low (low associates with foot of slope and soon the anomaly

recovers back to regional trend) is observed (Figure 2c). On close observation of gravity anomaly of the offshore part of the Krishna–Godavari Basin, it is found that the typical gravity low anomaly is altered with less amplitude and longer wavelength (see part of the Krishna–Godavari Basin region in Figure 5b). Gravity anomalies of the northern part of the margin have been modified due to sediment accumulations in Krishna–Godavari and Mahanadi basins.

We have discussed the results of ship-borne and various products of satellite geoid data for understanding the gravity signatures of various major and minor structural elements of the Bay of Bengal. Some of the key aspects include testing the volcanic origin of the 85°E Ridge and understanding its isostatic compensation in conjunction with the formation of adjacent lithosphere. Ship-borne gravity data will be studied in greater detail to understand how both ridges (85°E and Ninetyeast ridges), formed more or less similar processes in the Bay of Bengal and buried under 3 km thick sediment pile, show varied gravity signatures and compensation mechanisms. Two-dimensional quantitative model studies will be carried out to determine the crustal structures and elastic plate thicknesses below both the ridges and discussed with regard to response of adjacent lithosphere and pre-collision continental dense sediments in compensation of gravity anomalies.

1. Biswas, S. K., Rift basins in western margin of India and their hydrocarbon prospects with special reference to Kutch basin. *AAPG Bull.*, 1982, **66**, 1497–1513.
2. Majumdar, T. J., Mohanty, K. K. and Srivastava, A. K., On the utilization of ERS-1 altimeter data for offshore oil exploration. *Int. J. Remote Sensing*, 1998, **9**, 1953–1968.
3. Srivastava, A. K., Dodiwala, F., Majumdar, T. J. and Mohanty, K. K., ISRO–ONGC Joint Report, ONGC, Dehradun, 1995, p. 56.
4. Hwang, C., Hsu, H. Y. and Jang, R. J., Global mean surface and marine gravity anomaly from multi-satellite altimetry: application of deflection-geoid and inverse Vening Meinesz formulae. *J. Geodesy*, 2002, **76**, 407–418.
5. Majumdar, T. J. and Bhattacharyya, R., An atlas of very high-resolution satellite geoid/gravity over the Indian offshore. SAC Tech. Note No. SAC/RESIPA/MWRG/ESHD/TR-21/2004, Nov. 2004, p. 46.
6. Lundgren, B. and Nordin, P., Satellite altimetry – A new prospecting tool. Sixth Thematic Conference, Colorado, Environmental Research Institute of Michigan, Ann Arbor, Michigan, USA, 1988, pp. 565–575.
7. Wakker, K. F., Zandbergen, R. C. A., Van Geldorp, G. H. M. and Ambrosius, B. A. C., From satellite altimetry to ocean topography: a survey of data processing techniques. *Int. J. Remote Sensing*, 1988, **9**, 1797–1818.
8. Chapman, M. E., Techniques for interpretation of geoid anomalies. *J. Geophys. Res.*, 1979, **84**, 3793–3801.
9. Moritz, H., *Advanced Physical Geodesy*, Abacus Press, England, 1980, p. 500.
10. Farelly, B., The geodetic approximations in the conversion of geoid height to gravity anomaly by Fourier Transform. *Bull. Geod.*, 1991, **65**, 92–101.
11. Davis, J. C., *Statistics and Data Analysis in Geology*, John Wiley, New York, 1973, p. 550.
12. Norton, I. O. and Sclater, J. G., A model for the evolution of the Indian Ocean and the breakup of Gondwanaland. *J. Geophys. Res.*, 1979, **84**, 6803–6830.
13. Curray, J. R., Emmel, F. J., Moore, D. G. and Raitt, R. W., Structure, tectonics and geological history of the north eastern Indian Ocean. In *The Ocean Basins and Margins* (eds Nairn, A. E. M. and Stehli, F. G.), Plenum Press, New York, 1982, vol. 6, pp. 399–450.
14. Gopala Rao, D., Krishna, K. S. and Sar, D., Crustal evolution and sedimentation history of the Bay of Bengal since the cretaceous. *J. Geophys. Res.*, 1997, **102**, 17,747–17,768.
15. Gaina, C., Muller, R. D., Brown, B. and Ishihara, T., Micro-continent formation around Australia. In *The Evolution and Dynamics of the Australian Plate* (eds Hillis, R. and Muller, R. D.), Joint Geol. Soc. of Aust. Am. Spec. Pap., 2003, vol. 22, pp. 399–410.
16. McKenzie, D. P. and Sclater, J. G., The evolution of the Indian Ocean since the Late Cretaceous. *Geophys. J. R. Astron. Soc.*, 1971, **25**, 437–528.
17. Liu, C. S., Curray, J. R. and McDonald, J. M., New constraints on the tectonic evolution of the Eastern Indian Ocean. *Earth Planet. Sci. Lett.*, 1983, **65**, 331–342.
18. Krishna, K. S. *et al.*, Tectonic model for the evolution of oceanic crust in the northeastern Indian Ocean from the Late Cretaceous to the Early Tertiary. *J. Geophys. Res.*, 1995, **100**, 20011–20024.
19. Wiens, D. A. *et al.*, A diffuse plate boundary model for Indian Ocean tectonics. *Geophys. Res. Lett.*, 1985, **12**, 429–432.
20. Gordon, R. G., DeMets, C. and Argus, D. F., Kinematic constraints on distributed lithospheric deformation in the equatorial Indian Ocean from present-day motion between the Australian and Indian plates. *Tectonics*, 1990, **9**, 409–422.
21. Krishna, K. S., Ramana, M. V., Gopala Rao, D., Murthy, K. S. R., Malleswara Rao, M. M., Subrahmanyam, V. and Sarma, K. V. L. N. S., Periodic deformation of oceanic crust in the central Indian Ocean. *J. Geophys. Res.*, 1998, **103**, 17859–17875.
22. Krishna, K. S., Bull, J. M. and Scrutton, R. A., Evidence for multiphase folding of the central Indian Ocean lithosphere. *Geology*, 2001, **29**, 715–718.
23. Rao, T. C. S. and Bhaskara Rao, V., Some structural features of the Bay of Bengal. *Tectonophysics*, 1986, **124**, 141–153.
24. Baksi, A. K., Barman, T. R., Paul, D. K. and Farrar, E., Widespread early cretaceous flood basalt volcanism in eastern India: Geochemical data from the Rajmahal–Bengal–Sylhet Traps. *Chem. Geol.*, 1987, **63**, 133–141.
25. Ramana, M. V. *et al.*, Mesozoic anomalies in the Bay of Bengal. *Earth Planet. Sci. Lett.*, 1994, **12**, 469–475.
26. Murthy, K. S. R., Rao, T. C. S., Subrahmanyam, A. S., Malleswara Rao, M. M. and Lakshminarayana, S., Structural lineaments from the magnetic anomaly maps of the eastern continental margin of India (ECMI) and NW Bengal Fan. *Mar. Geol.*, 1993, **114**, 171–183.
27. Krishna, K. S. and Gopala Rao, D., Abandoned Paleocene spreading center in the northeastern Indian Ocean: Evidence from magnetic and seismic reflection data. *Mar. Geol.*, 2000, **162**, 215–224.
28. Subrahmanyam, C., Thakur, N. K., Gangadhara Rao, T., Khanna, R., Ramana, M. V. and Subrahmanyam, V., Tectonic of the Bay of Bengal: new insights from satellite-gravity and ship-borne. *Earth Planet. Sci. Lett.*, 1999, **171**, 237–251.
29. Krishna, K. S., Gopala Rao, D., Subba Raju, L. V., Chaubey, A. K., Shcherbakov, V. S., Pilipenko, A. I. and Radhakrishna Murthy, I. V., Paleocene on spreading axis hotspot volcanism along the Ninetyeast Ridge: An interaction between the Kerguelen hotspot and the Wharton spreading center. *Proc. Indian Acad. Sci. Earth Planet. Sci.*, 1999, **108**, 255–267.
30. Krishna, K. S., Neprochnov, Y. P., Gopala Rao, D. and Grinko, B. N., Crustal structure and tectonics of the Ninetyeast ridge from seismic and gravity studies. *Tectonics*, 2001, **20**, 416–433.

31. Krishna, K. S., Structure and evolution of the Afanasy Nikitin seamount, buried hills and 85 degrees E Ridge in the northeastern Indian Ocean. *Earth Planet. Sci. Lett.*, 2003, **209**, 379–394.
32. Rapp, R. H., The determination of geoid undulations and gravity anomalies from Seasat Altimeter. *J. Geophys. Res.*, 1983, **88**, 1552–1562.
33. Rajesh, S. and Majumdar, T. J., Generation of 3-D Geoidal surface of the Bay of Bengal lithosphere and its tectonic implications. *Int. J. Remote Sensing*, 2004, **25**, 2897–2902.
34. Subrahmanyam, V., Krishna, K. S., Radhakrishna Murthy, I. V., Sarma, K. V. L. N. S., Maria Desa, Ramana, M. V. and Kamesh Raju, K. A., Gravity anomalies and crustal structure of the bay of Bengal. *Earth Planet. Sci. Lett.*, 2001, **192**, 447–456.
35. Curray, J. R., Emmel, F. J. and Moore, D. G., The Bengal Fan: morphology, geometry, stratigraphy, history and processes. *Mar. Pet. Geol.*, 2003, **19**, 1191–1223.
36. Fu, L. L., Chelton, D. B. and Zlotnicki, V., Satellite altimetry: Observing ocean variability from space. *Oceanography*, 1988, **1**, 58.

ACKNOWLEDGEMENTS. We thank Prof. C. Hwang, National Chiao Tung University, Taiwan for providing high-resolution geoid/gravity data and related software. We also thank Dr K. N. Shankara, Director, SAC; Dr S. R. Shetye, Director, NIO; Dr K. L. Majumder, Dy. Director, RESIPA/SAC and Dr S. R. Nayak, Group Director, MWRG/RESIPA/SAC for their keen interest in this study. We thank the two anonymous reviewers whose comments and suggestions have helped improve the manuscript. This is NIO Contribution No. 4030.

Received 7 June 2005; revised accepted 4 October 2005

Fibre Bragg grating-based sensing device for petrol leak detection

Nahar Singh*, Subhash C. Jain, Vandana Mishra, G. C. Poddar, Palvinder Kaur, Himani Singla, A. K. Aggarwal and Pawan Kapur

Central Scientific Instruments Organisation, Sector 30, Chandigarh 160 030, India

Fibre Bragg gratings (FBGs) have emerged in recent years as important sensor elements for various applications. In this communication application of an FBG sensor using a surgical rubber as transducer element for petrol leak detection in pipelines and tanks is presented. The rubber, which is in tubular form and is bonded with the fibre containing FBG, reversibly swells in the presence of petrol thus resulting in Bragg wavelength shift. The shift is measured using an interrogator with a swept fibre laser source (1520–570 nm). The design aspects and experimental procedure along with analysis of results obtained and the potential for distributed sensing have been discussed.

Keywords: FBG sensor, petrol leak, transducer.

FIBRE Bragg gratings (FBGs) are simple intrinsic devices which are created in the fibre core by imaging an interfer-

ence pattern through the side of the fibre¹. They have all the advantages of an optical fibre, such as electrically passive operation, lightweight, high sensitivity and also some unique features of their own such as self-referencing and multiplexing capabilities, giving them a distinct edge over previously used devices. They are being used in structural health monitoring (SHM) of different types of civil structures, aircraft and aerospace vehicles^{2–4}. In all such applications, FBGs are used as strain and temperature sensors because these two parameters have direct influence upon the Bragg wavelength and also because they are important for SHM studies. However, the application potential of FBG sensors can reach new horizons by introducing transducers in combination with the grating element. The purpose of the transducer is to produce strain or temperature variation due to the parameter to be detected. This variation in any sensing parameter is detected by monitoring Bragg wavelength shift. This communication discusses one such application of FBG sensors for petrol leak detection. Since petrol is a hazardous and precious commodity, it can be both dangerous as well as an economic loss if it leaks through pipelines and tanks. FBG sensors are functional in such situations because they are insulators, chemically inert and perform multipoint sensing within a single fibre. A fast detection system of petrol leak along with its location is possible using FBG sensors. The results obtained have been discussed and analysed.

When a light wave passing through the fibre core comes across refractive index variation (which acts as a grating plane), it gets scattered. Most of the scattered light becomes more and more out of phase after passing through subsequent grating planes, cancelling out each other eventually. However, one particular wavelength which satisfies the Bragg condition, and hence called Bragg wavelength, undergoes scattering from subsequent grating planes and is in phase resulting in a constructive interference. This wavelength element thus is missing from the transmission and results in reflection. It is a function of grating parameters and is given by

$$I_B = 2n\Lambda, \quad (1)$$

where Λ is the pitch of the grating, n is the effective refractive index of the core and I_B is the Bragg wavelength⁵. As evident from eq. (1), the Bragg wavelength is shifted if the effective refractive index or the grating periodicity is changed due to some perturbation; in fact both these parameters are directly influenced by strain and ambient temperature. At a constant temperature, the effect of strain on the wavelength is given as

$$\Delta I_B = 2 \left[\Lambda \frac{\partial n}{\partial l} + n \frac{\partial \Lambda}{\partial l} \right] \Delta l. \quad (2)$$

In eq. (2), the first term is for change in refractive index of the core, induced due to strain optic effect, while the

*For correspondence. (e-mail: nsmehla@rediffmail.com)